Eng. & Tech. Journal, Vol. 28, No.7, 2010

Image Compression Based on 2D Dual Tree Complex Wavelet Transform (2D DT-CWT)

Dr. Salih Husain Ali * & Aymen Dawood Salman

Received on:1/7/2009
Accepted on:7/1/2010

Abstract

By removing the redundant data, the image can be represented in a smaller number of bits and hence can be compressed. There are many different methods of image compression. This paper investigates a proposed form of compression based on 2D Dual Tree complex wavelet transform (2D DT-CWT). Many wavelet coefficients are closed to zero. Thresholding can modify the coefficients to produce more zeros that are allowed a higher compression rate. The wavelet analysis does not actually compress a signal. Therefore Huffman coding is used with a signal processed by the wavelet analysis in order to compress data. Wide range of threshold values is used in the proposed form. From the results the proposed form give higher rate of compression and lower RMS error compared with that forms based on Discrete Wavelet Transform (DWT), Dual Tree Real Wavelet Transform (DT-RWT) and the well known method based Discrete Cosine Transform (DCT).

Keywords: Wavelet, Complex Wavelet Transform, Image Compression, Dual Tree Complex Wavelet Transform.

ضغط الصور بالآعتماد على التحويل المويجي المركب ثنائي الإبعاد ذي الشجرة الثنائية

الخلاصة

يمكن تمثيل الصورة بأقل عدد من البايتات بإزالة البيانات الفائضه. وبذلك سيتم ضغط الصورة. وهناك عدة طرائق لضغط الصورة. استخدمت في هذا البحث طريقة مقترحة تعتمد على التحويل المويجي المركب ثنائي الإبعاد ذي الشجرة الثنائية (2D DT-CWT) لضغط الصورة. العديد من المعاملات الخاصة بتحليل المويجي تقترب قيمتها من الصفر. من الممكن تعديل هذه المعاملات وتقريبها للصفر باستخدام العتبة (threshold) لنحصل على نسبة ضغط أعلى. ولايعتبر التحليل المويجي هو كاف لضغط البيانات ويستخدم معه ترميز هوفمان (Huffman Coding) لتحسين نسبة الضغط وتم استخدام مدى واسع من قيم العتبة في الطريقة المقترحة وتبين من النتائج إن الطريقة المقترحة تعطي نسبة ضغط عالية ونسبة خطاء قليلة (RMS error) بمقارنتها مع (DWT) وطريقة (DT-RWT) والطريقة المعروفة المعتمدة على (DCT).

***Computer Engineering & Information Technology, Department , University of Technology / Baghdad**

https://doi.org/10.30684/etj.28.7.2
2412-0758/University of Technology-Iraq, Baghdad, Iraq

1. Introduction

A typical still image contains a large amount of spatial redundancy in plain areas where adjacent picture elements (pixels, pels) have almost the same values. It means that the pixel values are highly correlated. The redundancy can be removed to achieve compression of the image data. The basic measure for the performance of a compression algorithm is compression ratio (CR), defined as a ratio between original data size and compressed data size. In a lossy compression scheme, the image compression algorithm should achieve a tradeoff between compression ratio and image quality. Higher compression ratios will produce lower image quality and vice versa. Quality and compression can also vary according to input image characteristics and content [1].

In recent years, many studies have been made on wavelets. Image compression is one of the most visible applications of wavelets. The rapid increase in the range and use of electronic imaging justifies attention for systematic design of an image compression system and for providing the image quality needed in different applications[1].

Although the discrete wavelet transform (DWT) has dominated the field of image compression for well over a decade, DWTs in their traditional critically sampled form are known to be somewhat deficient in several characteristics, lacking such properties as shift invariance and significant directional selectivity [2].

2. Complex Wavelet

The critically sampled discrete wavelet transform (DWT) has been successfully applied to a wide range of signal processing tasks. However, its performance is limited because of the following problems [2].

- Oscillations of the coefficients at a singularity (zero crossings).
- Shift variance when small changes in the input cause large changes in the output.
- Aliasing due to down-sampling and non-ideal filtering during the analysis, which is cancelled out by the synthesis filters unless the coefficients are not altered.
- Lack of directional selectivity in higher dimensions, e.g. inability to distinguish between $+45^o$ and -45^o edge orientations.

To overcome the shift dependence problem, they can exploit the undecimated (over-complete) DWT, however, without solving the directional selectivity problem. Another approach is inspired by the Fourier transform, whose magnitude is shift invariant and the phase offset encodes the shift. In such a wavelet transform, a large magnitude of a coefficient implies the presence of a singularity while the phase signifies its position within the support of the wavelet. The complex wavelet transform (CWT) employs *analytic* or *quadrature* wavelets guaranteeing magnitude-
phase representation, shift invariance and no aliasing [2].

Recently, complex-valued wavelet transforms CWT have been proposed to improve upon these DWT deficiencies, with the dual-tree CWT (DT-CWT) [3] becoming a preferred approach due to the ease of its implementation. In the DT-CWT, real valued wavelet filters produce the real and imaginary parts of the transform in parallel decomposition trees, permitting exploitation of well-established real-valued wavelet implementations and methodologies. A primary advantage of the DT-CWT lies in that it results in decomposition with a much higher degree of directionality than that possessed by the traditional DWT. However, since both trees of the DT-CWT are themselves orthonormal or biorthogonal decompositions, the DT-CWT taken as a whole is a redundant tight frame [2].

An analytic wavelet $y_c(t)$ is composed of two real wavelets $y_r(t)$ and $y_i(t)$ forming a Hilbert transform (HT) pair which means that they are orthogonal, i.e. shifted by $p/2$ in the complex plain [4].

$$y_c(t) = y_r(t) + j y_i(t) \quad \text{..... (1)}$$

$$y_i(t) = HT\{y_r(t)\} = \frac{1}{p}\int_{-\infty}^{\infty} \frac{y_r(t)}{t-t} dt = y_r(t) \frac{1}{p \quad t} \quad \text{.....(2)}$$

And for their Fourier transform pairs $H_r(w)$ and $H_i(w)$.

$$H_i(w) = FT\{HT\{y_r(t)\}\} = -j.\text{sgn}(w) H_r(w) \quad \text{.....(3)}$$

The same concept of analytic or quadrature formulation is applied to the filter bank structure of standard DWT to produce complex solutions and in turn the CWT. The real-valued filter coefficients are replaced by complex-valued coefficients by proper design methodology that satisfies the required conditions for convergence. Then the complex filter can again be decomposed into two real-valued filters. Thus, two real-valued filters that give their respective impulse responses in quadrature will form the Hilbert transform pair. The combined pair of two such filters is termed as an analytic filter. The formulation and interpretation of the analytic filter is shown in figure (1) [4].

2.1 1D Dual-Tree CWT

Similarly to the DWT, the DT-CWT is a multiresolution transform with decimated subbands providing perfect reconstruction of the input. In contrast, it uses analytic filters instead of real ones and thus overcomes problems of the DWT at the expense of moderate redundancy. Running in two DWT trees a and b (real and imaginary) of real filters, this transform produces real and imaginary parts of the coefficients.

The wavelet functions $y_r(t)$ and $y_i(t)$ producing the complex wavelet $y_c(t)$ form an approximate HT pair. The same applies to the scaling functions $f_r(t)$ and $f_i(t)$. The wavelet and scaling functions are related to the corresponding filters through the dilation and wavelet equations [5].

$$y(t) = \sqrt{2}\sum_n h_1(n) f(2t-n) \quad \text{.....(4)}$$

$$f(t) = \sqrt{2}\sum_n h_0(n) f(2t-n) \quad \text{.....(5)}$$

where t denotes continuous time and n the discrete time index

The half-sample delay condition is derived from a strategy of designing filters so that the wavelets generated by them form the Hilbert transform pair. This happens when the scaling filters h_0 and g_0 are offset from one another by a half sample.

$$g_0(n) = h_0(n - 0.5) \quad \ldots\ldots(6)$$

As a result, the lowpass filters of one tree interpolate midway between the lowpass filters of the other tree and the DT-CWT is shift invariant. In the frequency domain, the magnitude condition is given by.

$$\left|G_0(e^{jw})\right| = \left|H_0(e^{jw})\right| \quad \ldots\ldots.(7)$$

And the phase condition runs [2].

$$\angle G_0(e^{jw}) = \angle H_0(e^{jw}) - 0.5w \ldots (8)$$

The filterbank structures for both DT-CWT are identical. Figure (2) shows 1-D analysis and synthesis filterbanks spanned over three levels. It is evident from the filterbank structure of DT-CWT that it resembles the filterbank structure of standard DWT with twice the complexity. It can be seen as two standard DWT trees operating in parallel. One tree is called as a real tree and other is called as an imaginary tree. Sometimes in future discussions the real tree will be referred to as *tree-a* and the imaginary tree as *tree*-b.

The form of conjugate filters used in 1-D DT-CWT is given as $(h_x + jg_x)$ where, h_x is the set of filters $\{h_0, h_1\}$, and g_x is the set of filters $\{g_0, g_1\}$ both sets in only x-direction (1-D). The filters h_0 and h_1 are the real-valued lowpass and highpass filters respectively for real tree. The same is true for g_0 and g_1 for imaginary tree.

Though the notation of h_0 and h_1 are use for all level in the real part of analysis tree, h_0 and h_1 of first level are numerically different then the respective filters at all other levels above level-1. The same notion is applied for imaginary tree filters g_0 and g_1. The synthesis filter pairs $\tilde{h}_0, \tilde{h}_1$, and $\tilde{g}_0, \tilde{g}_1$ as shown in figure (2 b) form orthogonal or biorthogonal pairs with their respective counterpart filters of analysis tree as shown in figure (2 a).

2.2 2D DT-CWT

Apart from that, the 2D DT-CWT also more selectively discriminates features of various orientations. While the critically decimated 2D DWT outputs three orientational selective sub-bands per level conveying image features oriented at the angles of 90^o, $\pm 45^o$, and 0^o, the 2D DT-CWT produces six directional subbands per level to reveal the details of an image in $\pm 15^o$, $\pm 45^o$ and $\pm 75^o$ directions with 4:1 redundancy [6].

The implementation of 2-D DT-CWT consists of two steps. ***Firstly,*** an input image is decomposed up to a desired level by two separable 2-D DWT branches, branch *a* and branch *b*, whose filters are specifically designed to meet the Hilbert pair requirement. Then six high-pass subbands are

generated:

$HL_a, LH_a, HH_a, HL_b, LH_b,$ and HH_b , at each level. ***Secondly,*** every two corresponding subbands which have the same pass-bands are linearly combined by either averaging or differencing. As a result, subbands of 2-D DT-CWT at each level are obtained as $(LH_a + LH_b)/\sqrt{2}$,

$(LH_a - LH_b)/\sqrt{2}$,

$(HL_a + HL_b)/\sqrt{2}$,

$(HL_a - HL_b)/\sqrt{2}$,

$(HH_a + HH_b)/\sqrt{2}$,

$(HH_a - HH_b)/\sqrt{2}$.

The six wavelets defined by oriented, as illustrated in figure (3). Because the sum/difference operation is orthonormal; this constitutes a perfect reconstruction wavelet transform. The imaginary part of 2D DT-CWT has similar basis function as the real part [8].

The 2-D DT-CWT structure has an extension of conjugate filtering in 2-D case. The filterbank structure of 2-D dual-tree is shown in figure (4). 2-D structure needs four trees for analysis as well as for synthesis. The pairs of conjugate filters are applied to two dimensions (x and y) directions, which can be expressed as:

$$(h_x + jg_x)(h_y + jg_y) = (h_x h_y - g_x g_y) + j(h_x g_y + g_x h_y) \quad \text{.....(9)}$$

The filterbank structure of *tree-a*, similar to standard 2-D DWT spanned over 3-level, is shown in figure (5). All other *trees-(b,c,d)* have similar structures with the appropriate combinations of filters for row- and column- filtering. The overall 2-D dual-tree structure is 4-times redundant (expensive) than the standard 2-D DWT. The *tree-a* and *tree-b* form the real pair, while the *tree-c* and *tree-d* form the imaginary pair of the analysis filterbank. Trees-($\tilde{a}$, $\tilde{b}$) and trees-($\tilde{c}$, $\tilde{d}$) are the real and imaginary pairs respectively in the synthesis filterbank similar to their corresponding analysis pairs [4].

3. Image Compression

Images require much storage space, large transmission bandwidth and long transmission time. The only way currently to improve on these resource requirements is to compress images, such that they can be transmitted quicker and then decompressed by the receiver.

There are many different methods of data compression. This investigation will concentrate on transform coding and then more specifically on Wavelet Transforms. Image data can be represented by coefficients of discrete image transforms. Coefficients that make only small contributions to the information contents can be omitted. Usually the image is split into blocks (subimages) of 8x8 or 16x16 pixels, then each block in discrete cosine transform is transformed separately. However this does not take into account any correlation between blocks, and creates "blocking artifacts" , which are not good if a smooth image is required.

However wavelets transform is applied to entire images, rather than subimages, so it produces no blocking artifacts. This is a major advantage of

wavelet compression over other transform compression methods.

For some signals, many of the wavelet coefficients are close to or equal to zero. Thresholding can modify the coefficients to produce more zeros. In Hard thresholding any coefficient below a threshold λ, is set to zero. This should then produce many consecutive zero's which can be stored in much less space, and transmitted more quickly by using entropy coding compression.

An important point to note about Wavelet compression is "The use of wavelets and thresholding serves to process the original signal, but, to this point, no actual compression of data has occurred".

This explains that the wavelet analysis does not actually compress a signal, it simply provides information about the signal which allows the data to be compressed by standard entropy coding techniques, such as Huffman coding. Huffman coding is good to use with a signal processed by wavelet analysis, because it relies on the fact that the data values are small and in particular zero, to compress data. It works by giving large numbers more bits and small numbers fewer bits. Long strings of zeros can be encoded very efficiently using this scheme. Therefore an actual percentage compression value can only be stated in conjunction with an entropy coding technique. To compare different wavelets, the number of zeros is used. More zeros will allow a higher compression rate, if there are many consecutive zeros, this will give an excellent compression rate.

There are two thresholding methods frequently used. The *soft-threshold* function (also called the shrinkage function) is shown in figure (6 a).

$$h_T(x) = \mathrm{sgn}(x).\max(|x| - T, 0) \quad \text{.....(10)}$$

takes the argument and shrinks it toward zero by the threshold T. The other popular alternative is the *hard-threshold* function is shown in figure (6 b).

$$y_T(x) = x\{|x| > T\} \quad \text{..... (11)}$$

which keeps the input if it is larger than the threshold T; otherwise, it is set to zero. The wavelet thresholding procedure removes noise by thresholding *only* the wavelet coefficients of the detail subbands, while keeping the low resolution coefficients unaltered [9].

3.1 Compression Algorithm

The different method for compression, investigate differ only in the selection of the method. The basic procedure remains the same:

(1) Digitise the source image into a signal.
(2) Decompose the signal s into wavelet coefficients using DT-CWT.
(3) Modify the coefficients from w, using thresholding.
(4) Apply variable length coding (Huffman coding) to compress.
(5) Reconstruct using the original approximation coefficients using inverse DT-CWT.

Figure (7) illustrates that the compression algorithm using DT-CWT.

4. Experimental Results and Discussions

Many standard files of images (lena, monarch, lmess and stone) are taken in this paper to know the strong and weak sides of the proposed method. Another methods such as image compression based DWT, 2D DT-RWT and the well known method (image compression based DCT) are implemented for the standard files of images that mentioned above.

Table (1) represents the result of compression ratio and RMS error for may standards images, each image is compressed by using the compression methods based on DWT,2D-DTRWT, DCT and the proposed form that based 2D DT-CWT. The proposed method give higher rate of compression and lower RMS error compared with other methods for many standard methods.

The various methods of compression are affected by threshold value. High values of threshold give higher rate of compression. From Table (1), it is clear that the different method of compression gives the same compression ratio for different values of thresholds. For example when lena image is compressed the compression ratio is (25:1), the thresholds values equals to 65, 50, 35 and 23 for the methods based DCT, DWT, 2D DT-RWT and 2D DT-CWT respectively. Hence the lena compressed image as shown in figure (8) is more smoothing and have lower RMS error when the method based 2D DT-CWT is used. The results of various methods are explained in figure (9) with the same threshold value (T=40) for lena image.

Figure (10) illustrates that the compression ratio is improved with increasing the threshold value. On the other hand the RMS error value is increased when the compression rate (CR) is increased as shown in figure (11).

5. Conclusions

Various methods of image compression based wavelet techniques are affected by threshold values until the proposed. Image compression scheme using 2D Dual Tree Complex Wavelet Transform (DT-CWT). For the same compression ratio the compressed image using proposed form is more smoothing and have lower RMS error compared with other methods based wavelet techniques and DCT technique. For certain value of threshold the proposed form based 2D DT-CWT give higher rate of compression and lower RMS error compared with that forms based on DWT, DT-RWT and method based (DCT).

References

[1] S. Grgic and M. Grgic, **"Performance Analysis of Image Compression Using Wavelet",** IEEE Transaction on Industrial Electronics, Vol. 48, No. 3, June 2001.

[2] I. W. Selesnick, R. G. Baraniuk, and N. G. Kingsbury, **"The dual-tree complex wavelet transform,"** IEEE Signal Processing Magazine, vol. 22, no. 6, pp. 123–151, November 2005.

[3] N. G. Kingsbury, **"Complex wavelets for shift invariant analysis and filtering of signals,"** Journal of Applied Computational

Harmonic Analysis, vol. 10, pp. 234– 253, May 2001.

[4] P. D. Shukla. **"Complex Wavelet Transforms and Their Applications,"** PhD thesis, The University of Strathclyde in Glasgow, 2003.

[5] I. W. Selesnick. **"Hilbert Transform Pairs of Wavelet Bases,"** IEEE Signal Processing Letters, 8(6):170-173, June 2001.

[6] E. Hostalkova, A. Prochazka **"Hilbert Transform Pairs of Wavelet Bases," internet**.

[7] J. Yang, J. Xu, F. Wu, Q. Dai, and Y.Wang. **"Image Coding Using 2D Anisotropic Dual Tree Discrete Wavelet Transform" IEEE 2007**.

[8] K. Lees. **" Image Compression Using Wavelets" May 2002.** http://web.cecs.pdx.edu/~mperkows/CAPSTONES/HAAR/u9kvl.pdf

[9] N. Jacob and A. Martin, "**Image Denoising In The Wavelet Domain Using Wiener Filtering",** http://homepages.cae.wisc.edu/~ece533/project/f04/jacob_martin.pdf

Table (1) RMS values of compressed images for different test images and CR

Image	CR	8X8 DCT		DWT		DT-RWT		DT-CWT	
		Mim RMS err	Thres hold	Mim RMS err	Thres hold	Mim RMS err	Thres hold	Mim RMS err	Thres hold
lena	5:1	4.6272	20	3.0177	15	2.4351	10	1.5098	5
	10:1	6.1767	35	4.1895	25	3.848	20	206076	10
	15;1	6.9731	45	4.9746	35	4.3732	25	3.4164	15
	20:1	7.6084	55	5.6639	45	4.8111	30	4.0228	20
	25:1	8.1978	65	5.9773	50	5.1837	35	4.2107	23
monarch	5:1	8.1441	35	4.685	25	3.545	18	2.6321	10
	10:1	11.0752	62	6.8725	43	5.9227	32	4.2126	19
	15;1	12.1864	90	8.2769	65	7.0249	43	5.4356	27
	20:1			9.2953	79	8.2431	55	6.448	35
	25:1			10.4014	95	8.9862	65	7.193	42
lmees	5:1	4.3464	23	3.3405	17	2.6194	12	1.9852	6
	10:1	6.6818	41	4.9963	31	3.8738	21	2.9852	13
	15;1	7.9831	56	5.9018	45	4.7133	30	3.2054	19
	20:1	8.8992	70	6.684	56	5.2927	39	4.019	24
	25:1	9.567	82	7.315	64	6.1909	46	4.5793	29
stone	5:1	6.1573	27	3.7314	17	3.4611	14	2.2958	7
	10:1	10.632	47	5.2433	31	4.6079	24	3.5521	12
	15;1	9.759	64	6.2244	45	5.5168	34	4.4025	20
	20:1	10.8199	80	7.032	55	6.2168	41	4.953	25
	25:1	11.395	92	7.7505	65	6.6273	49	5.3485	30

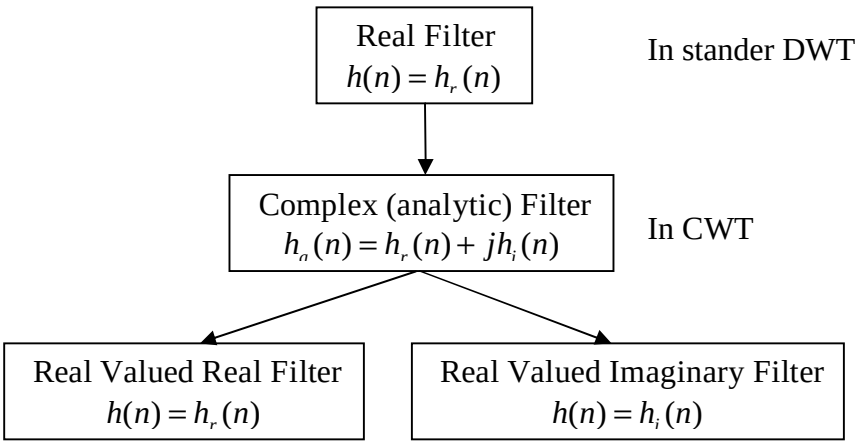

Figure (1) Interpretation of an analytic filter by 2-real filter [4].

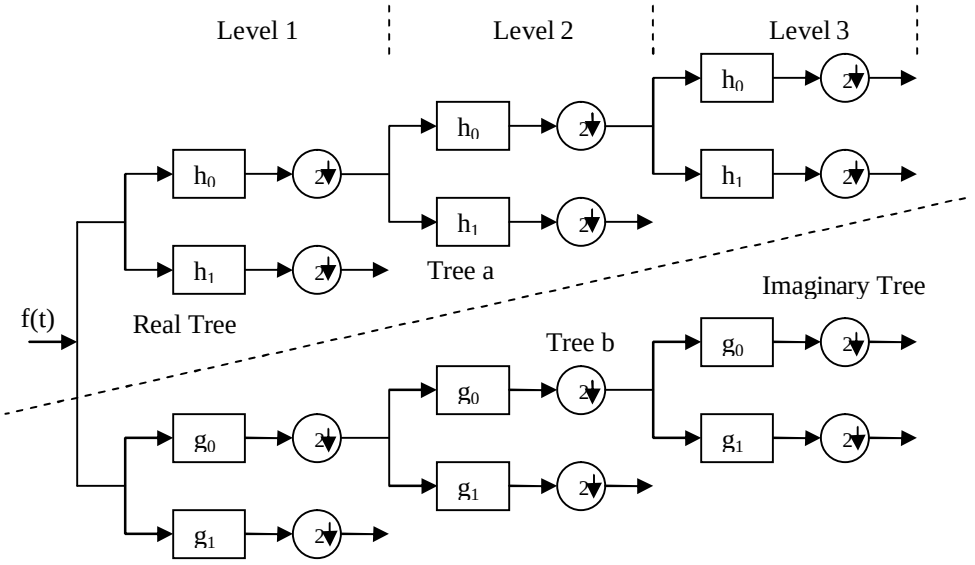

(a)

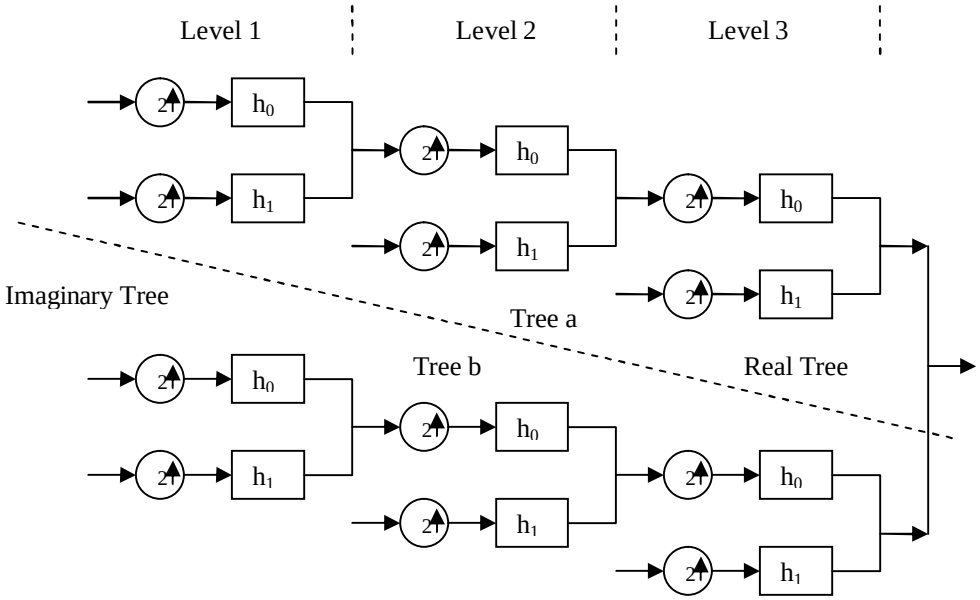

(b)

Figure (2) (a) Analysis (b) Synthesis filter bank for 1-D DT-CWT [4].

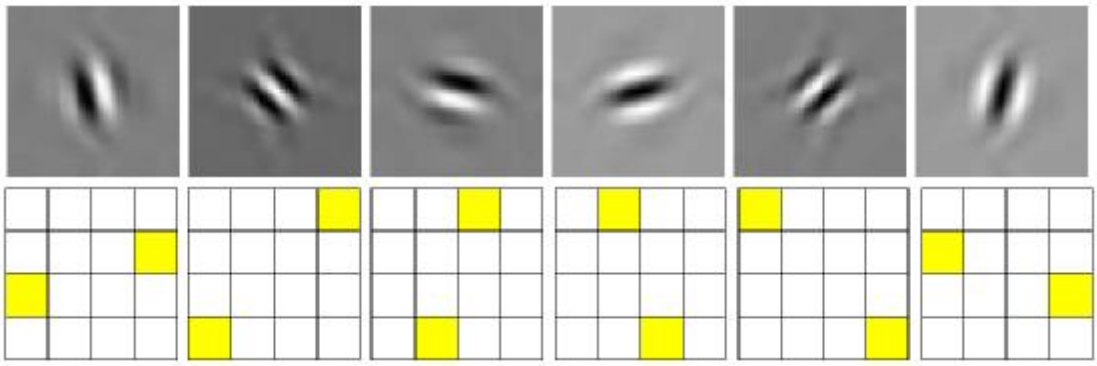

Figure (3) Typical wavelets associated with the 2-D dual-tree oriented wavelet transform. The top row illustrates the wavelets in the spatial domain, the second row illustrates the (idealized) support of the spectrum of each wavelet in the 2-D frequency plane [8]

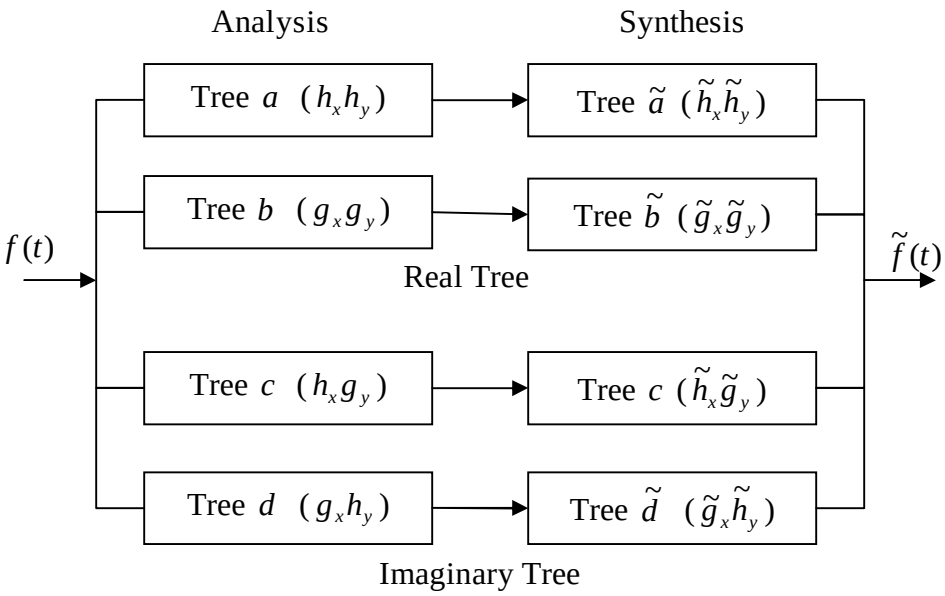

Figure (4) Filter bank structure for 2-D DT-CWT [4]

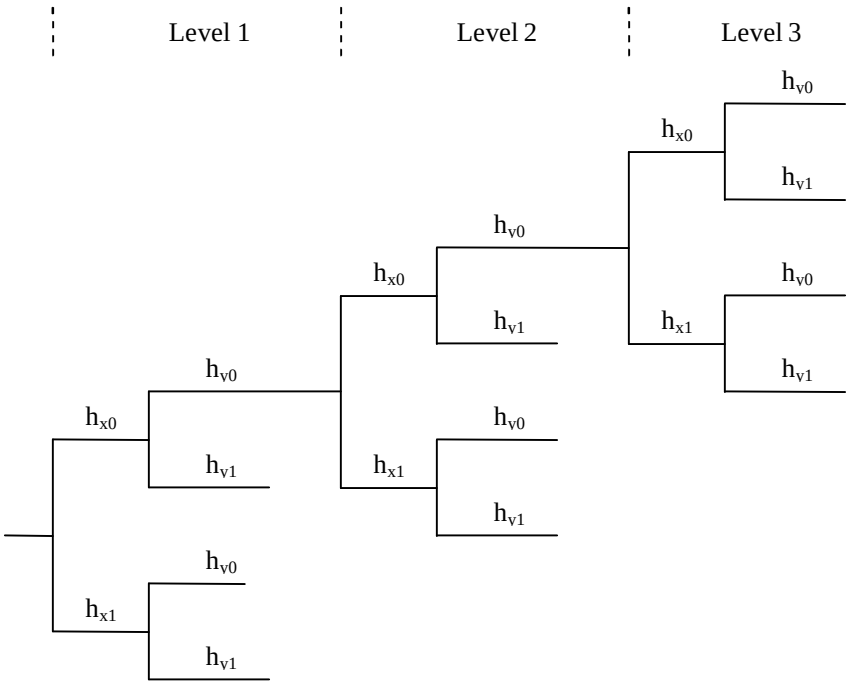

Figure (5) Filter bank structure of tree-a of figure (4) [4]

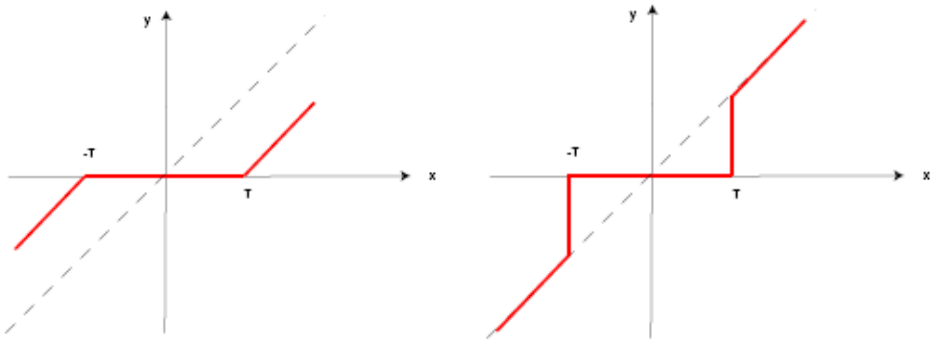

(a) (b)

Figure (6) (a) Soft Thresholding (b) Hard Thresholding [9].

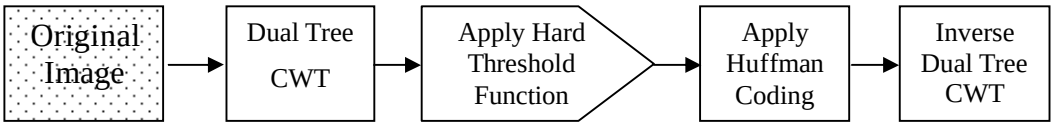

Figure (7) Image Compression structure using DT-CWT

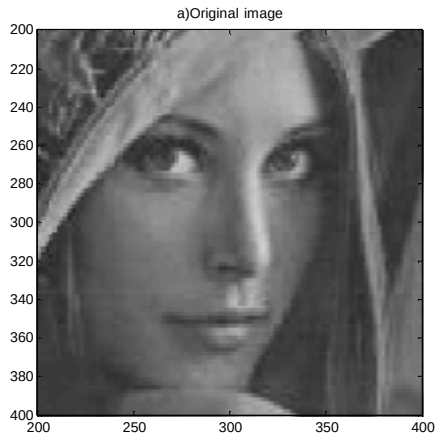

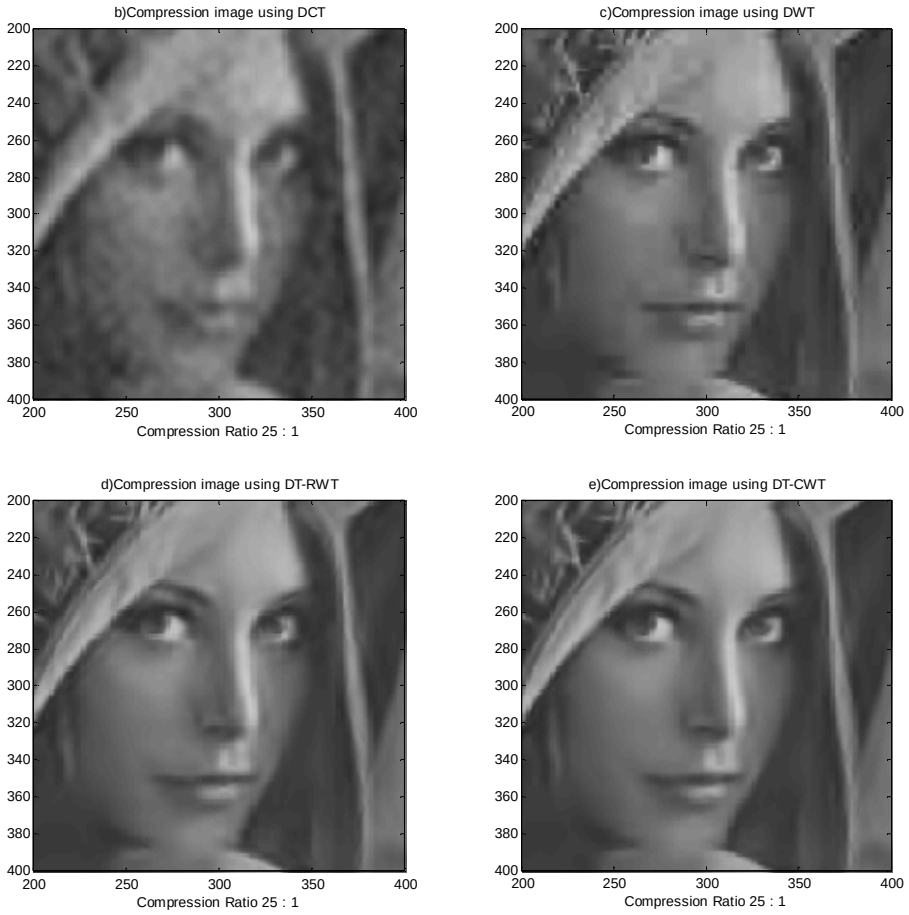

Figure (8) The performance of the various methods on lena.tif with compression ratio (25:1) (a) Original. (b) Compression image using DCT. (c) Compression image using DWT. (d) Compression image using DT-RWT. (e) Compression image using DT-CWT

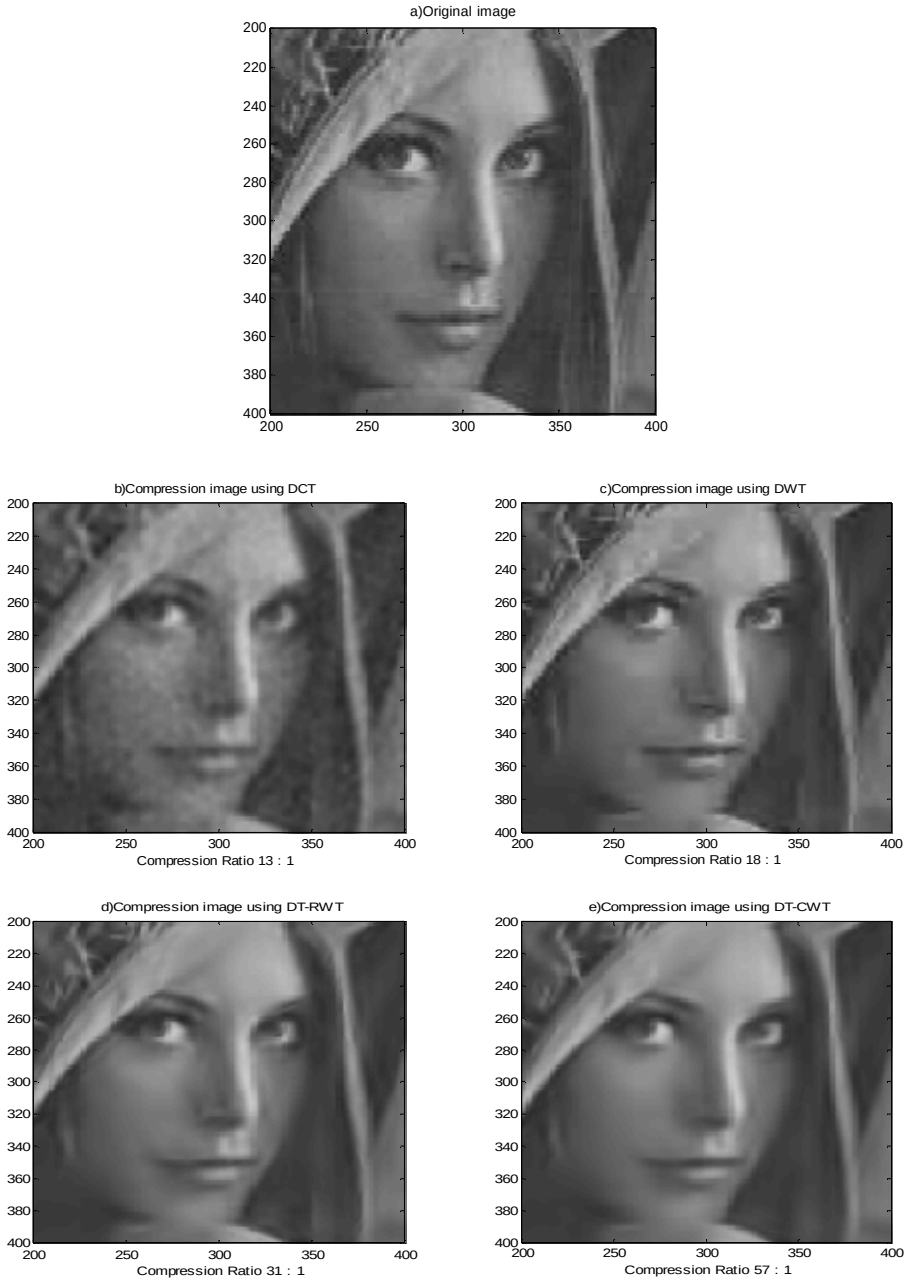

Figure (9) The performance of the various methods on lena.tif with threshold level (T=40). (a) Original. (b) Compression image using DCT. (c) Compression image using DWT. (d) Compression image using DT-RWT. (e) Compression image using DT-CWT

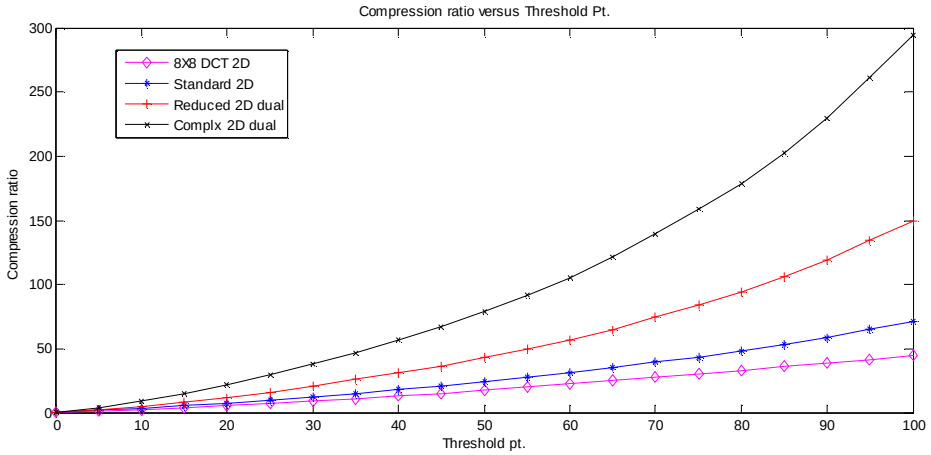

Figure (10) Illustrates Compression Ratio versus threshold points plot for lena.tif.

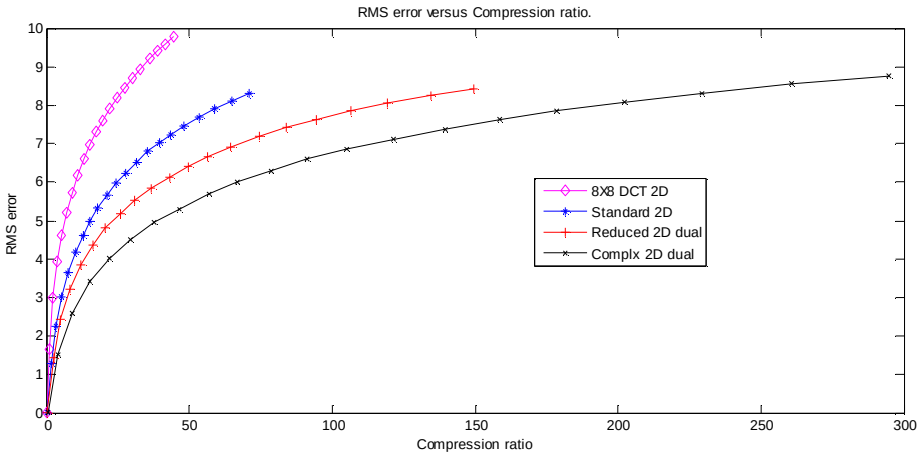

Figure (11) Illustrates RMS error versus Compression Ratio plot for lena.tif